

A sensitive nuclear quadrupole resonance spectrometer for 2-60 MHz

This article has been downloaded from IOPscience. Please scroll down to see the full text article.

1982 J. Phys. E: Sci. Instrum. 15 814

(<http://iopscience.iop.org/0022-3735/15/8/005>)

View [the table of contents for this issue](#), or go to the [journal homepage](#) for more

Download details:

IP Address: 132.198.151.69

The article was downloaded on 10/09/2010 at 18:34

Please note that [terms and conditions apply](#).

RESEARCH PAPERS

A sensitive nuclear quadrupole resonance spectrometer for 2–60 MHz

F N H Robinson

Clarendon Laboratory, University of Oxford, Parks Road, Oxford OX1 3PU

Received 11 January 1982, in final form 15 March 1982

Abstract. The paper describes the design, construction and performance of a continuous-wave spectrometer for use at temperatures between 77 K and 80°C. The limiting sensitivity for chlorine resonances with narrow lines is 1 μmol and compounds of molar volume up to 10⁴ cm³ can be studied. The corresponding figures for nitrogen resonances are 300 μmol and 10³ cm³. The continuous tuning range with a single coil is 2.5:1 and the resolution is a few PPM. It uses bisymmetric Zeeman modulation, there are no critical adjustments and no elaborate extra equipment is required.

1. Introduction

Although Fitzky (1974) has reported a signal-to-noise ratio of 5:1 obtained from 200 μmol of chlorine using a 10 s phase-sensitive detector (PSD) time constant, nuclear quadrupole resonance (NQR) spectrometry is reputed to be a relatively insensitive technique requiring large samples. Yet Pound (1950) in his pioneer paper gave a theoretical estimate of the s/N ratio which would suggest that sharp chlorine resonances ought to be observable with only one or two μmol . We shall describe an instrument which goes some way to closing the gap between the best current practice and theoretical expectation.

For a given resonance the sensitivity of a spectrometer depends on the Q of the coil and its filling factor and on the noise temperature of the oscillator and its capacity to drive enough RF voltage across the coil to approach saturation. These last two requirements conflict since low-noise circuits will not usually handle high RF voltages.

The super-regenerative oscillator gives a large voltage but, although it has some advantages in studying broad lines, it is difficult to see how a circuit operating in such a highly nonlinear mode can yield a low noise temperature. A marginal oscillator gives a low noise temperature if the loop gain is near unity and the feedback circuit is very nearly linear with a gain that falls slowly and monotonically with increasing amplitude. This is difficult to achieve over a wide range of levels and frequencies without continual critical adjustment. The limited oscillator (Robinson 1959) has the same low noise temperature as a properly adjusted marginal oscillator but does not need continual adjustment nor does it depend critically on the exact

characteristics of particular devices. On the other hand, unlike the super-regenerative and marginal oscillators it does not display an intrinsic amplification of both the signal and the noise arising from the way the amplitude of oscillation is determined by the nature of the feedback loop. As a result it also requires a low-noise detector. This is, however, a relatively straightforward design problem and so we have based our instrument on a limited oscillator circuit.

Frequency modulation presents insuperable problems of base-line drift, and spurious signals, in wide tuning-range circuits which are needed to search for new resonances. Provided that ferromagnetic contamination is rigorously excluded from the tank circuit the bisymmetric Zeeman modulation scheme with second-harmonic detection of Verwieck and Cornwell (1961) is free from this objection (Robinson 1980a). With a cw oscillator it has the further advantage that it gives very clear spectra with the chart-recorder trace representing the true absorption line rather than its derivative, even though the lines may occasionally display inverted wings whose origin has been discussed by Watkins and Pound (1952). The modulator we use has been described elsewhere (Robinson 1980b).

The oscillator circuit uses a long-tailed pair of bipolar transistors (Faulkner and Holman 1967) as the limiter, and these transistors also serve as a moderately efficient detector (Robinson 1974); however, in order to avoid loading the tuned circuit and degrading its Q the limiter is preceded by a broadband low-noise amplifier with a FET input stage. The gain in this amplifier minimises the influence of the moderate detector efficiency on the overall noise temperature and, at 30 MHz, the electronic contribution to this temperature is only about 200 K. It increases at higher frequencies but falls to negligible values at lower frequencies where, of course, sensitivity is most important.

The presence of this amplifier with a small, mainly capacitive, input admittance allows the tank circuit to be very loosely coupled, through a few picofarads, to the active electronics. As a result, very little RF current flows in the line from the tank circuit to the electronics and if the main tuning capacitor is placed near the coil in the cryostat, loss in this line has little effect on the Q nor does its stored magnetic energy reduce the effective sample filling factor. Both these factors improve the sensitivity.

The amplifier restricts the RF voltage that can be handled without overloading, especially at high frequencies, but nevertheless one can manage, without increasing the noise figure, amplitudes from 0.05 up to 2 V across the coil, even at 50 MHz, and this is sufficient to saturate most lines at 77 K, if not at room temperature. It is easy to increase the voltage at low frequencies but to do so at high frequencies would be more difficult.

The tuning capacitor is a modified 150 pF air-spaced trimmer and it is driven by a shaft passing through a simple

greased O ring seal at the head of the cryostat. Figure 1 shows the complete spectrometer with the worm-gear capacitor drive in place and a modulating coil attached to the tail. The top plate is maintained at $30 \pm 5^\circ\text{C}$ by a small thermostat. This prevents condensation on the RF lead where it passes through the top plate using a small press-fit PTFE leadthrough. There is also a lead to a diode thermometer, attached to the tank-circuit assembly, and a knob to operate a switch that inserts extra capacitance and extends the tuning range to 4:1. The small diecast box ($115 \times 60 \times 30$ mm) houses the printed circuit board (PCB) on which is mounted the oscillator circuit together with RF and LF buffer amplifiers and power lead filters. A coaxial cable leads directly from this box to a frequency counter and a 4-core screened cable leads to the power supply and eventually to the PSD. This cable also contains a lead which controls a varicap diode that can be used to give very slow band-spread tuning over a limited range. The DC voltage on the signal lead responds to the RF level and is used to operate a meter that can be calibrated by connecting a signal generator across the tank circuit. The overall length of the cryostat, from the tail to the top plate, is 280 mm, the tail diameter is 25 mm and the main tube diameter 50 mm.

The ancillary equipment required comprises the modulator, a PSD with a second-harmonic reference, a chart recorder, a frequency counter, a stabilised PSU giving ± 27 V at 30 mA and a motor to drive the capacitor, with a range of speeds from 10^{-3} to 10 RPM. Apart from tuning there is only one other control

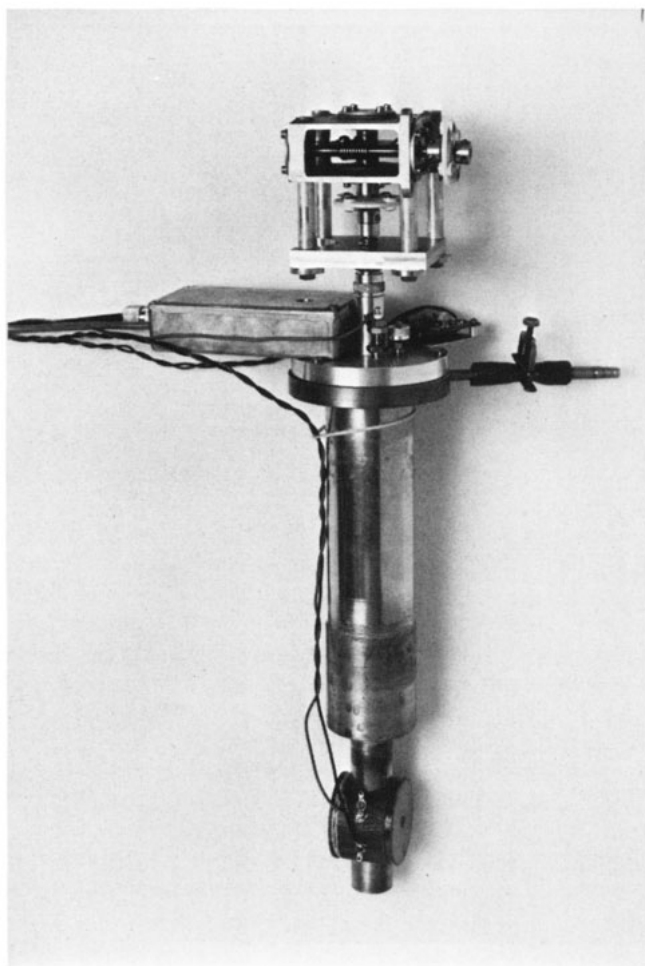


Figure 1. A general view of the spectrometer.

associated with the RF head, a small variable capacitor on the PCB which sets the RF level. Although no attempt has been made to stabilise the RF level, which therefore rises rather faster than linearly with increasing frequency, the level control can, at a slight loss in sensitivity near the ends of the scan, be left unadjusted over an octave scan (see figure 4) but it is preferable to reset it four or five times during a complete scan which usually means only once or twice a day. It is, in any case, desirable to have a level which rises linearly with frequency, as this maintains a constant saturation parameter.

Some of the results which can be obtained with this instrument are now presented and where numerical values for the s/N ratio are mentioned this will be in terms of the ratio of the peak signal height to a visual estimate of the RMS noise, since this is the ratio predicted by theory. The noise estimate is to some extent subjective and so the accuracy of these figures is probably worse than $\pm 25\%$.

2. Experimental spectra

Figure 2 shows the complex spectrum due to ^{35}Cl in carbon tetrachloride at 77 K. It illustrates the clarity and resolution of the spectra that can be obtained from samples approaching conventional size, in this case 0.6 cm^3 , or 1 g, of material. The PSD time constant is 10 s and the frequency markers are at 10 kHz intervals with wider markers every 100 kHz. Only the resolution of the chart recorder prevented the use of 1 kHz or finer markers.

Figure 3 shows lines obtained from a composite sample at 77 K containing $30\ \mu\text{mol}$ each of sodium chlorate (3 mg) and potassium chlorate (3.5 mg) in a small coil 8 mm long wound on a 2 mm diameter thin-walled PTFE tube. The upper traces show

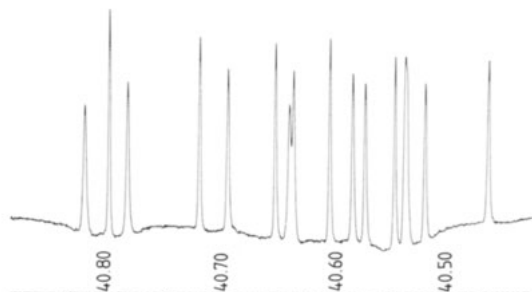


Figure 2. The spectrum of CCl_4 at 77 K near 40 MHz.

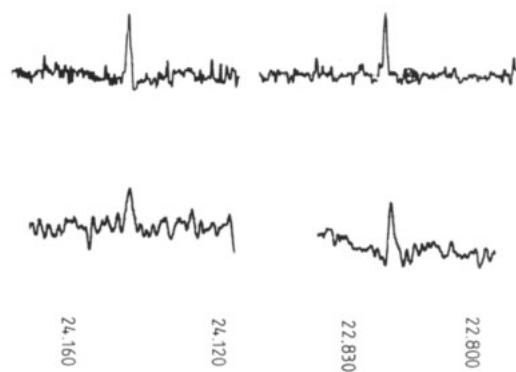


Figure 3. Lines due to ^{35}Cl and ^{37}Cl in $30\ \mu\text{mol}$ of sodium and potassium chlorate.

the ^{35}Cl lines with a 1 s PSD time constant and the lower traces show the ^{37}Cl lines with a 50 s time constant. Since the ^{37}Cl lines are six times less intense than the ^{35}Cl lines and the ratio of the square roots of the bandwidths is 7:1, we might have expected similar signal-to-noise ratios. In fact, the ^{35}Cl lines give 10:1 while the ^{37}Cl give only 5:1. The extra noise with the long time constant probably shows that we are approaching a limit set by the overall stability of the system. With a 10 s time constant the s/N ratio for ^{35}Cl is, as expected, 30:1 and corresponds to a limiting sensitivity of $1\ \mu\text{mol}$. The accessible sample volume within the coil former is $14\ \text{mm}^3$ and so we see that we could expect useful signals from as little as $10\ \mu\text{mol}$ of a compound of molar volume up to $1000\ \text{cm}^3$ (for purposes of comparison the molar volume of NaClO_3 is $40\ \text{cm}^3$).

Figure 4 shows some of the lines obtained at 77 K with a 1 s time constant during a continuous scan from 55 to 27 MHz made without adjusting the RF level. The self-supporting coil has an internal diameter of 10 mm and a length of 24 mm which gives a usable sample volume of over $1.5\ \text{cm}^3$ and it easily accommodates four separate specimen tubes containing: (i), 71 mg ($530\ \mu\text{mol}$) of N-chlorosuccinimide (NCS); (ii), 62 mg ($440\ \mu\text{mol}$ of chlorine per resolved line) of hexachlorobenzene (HCB); (iii), 27 mg ($370\ \mu\text{mol}$ of chlorine) of p-dichlorobenzene (PDCB); and (iv) 39 mg ($370\ \mu\text{mol}$) of sodium chlorate.

Line A, at 54.1 MHz is due to ^{35}Cl and line B at 42.6 MHz to ^{37}Cl in NCS. The three lines C near 38.4 MHz are due to ^{35}Cl in HCB. Lines D and F at 34.8 and 27.4 MHz are due to ^{35}Cl and ^{37}Cl in PDCB and line E is the 30.6 MHz ^{35}Cl line in sodium chlorate. Line G shows the improvement in line F that can be effected by re-adjusting the level at the end of the scan. From line A, at 54.1 MHz to line F at 27.4 MHz, the baseline drifts by about twice the height of the strong signals, which is easily within the range of the chart recorder.

The signal-to-noise ratio for line D is 15:1 from $370\ \mu\text{mol}$ of chlorine so that even with this short time constant the limiting sensitivity is $25\ \mu\text{mol}$ and useful signals would be available from compounds of molar volume up to $10^4\ \text{cm}^3$, say 500 carbon atoms per chlorine. We have not been able to check this directly but we have been able to study the phase change in cholesteryl chloride ($\text{C}_{27}\text{H}_{45}\text{Cl}$) between room temperature and 77 K. This is a very light fluffy wax with an effective density of less than $0.25\ \text{g cm}^{-3}$ giving a molar volume over $1600\ \text{cm}^3$. Furthermore the single broad line at $40\ ^\circ\text{C}$ splits into four lines each 8 kHz wide at 77 K so that we can certainly detect a rather broad line in a compound whose molar volume per resolved line is $6400\ \text{cm}^3$.

Although the signals shown in figure 4 obtained with a relatively fast sweep are enough to indicate the presence and frequencies of the lines, they are not clear enough to show their width and possible structure. Figure 5 therefore shows the improvement that can be made by using a longer time constant, 50 s, and a slower scan. The three lines from HCB can now be located and their widths measured to better than 1 kHz.

Although the spectrometer noise temperature and sensitivity deteriorate above 45 MHz, it is still usable up to 130 MHz and, with the aid of switched capacitance, we have (Weaver and Robinson 1981) been able to observe all four lines, from 30.6 to 119 MHz in the spectrum of ^{209}Bi at 77 K in triphenylbismuth without removing the sample or disturbing its temperature.

By changing a few passive components in the circuit, the basic oscillator which covers 15–60 MHz can be arranged to operate down to below 2 MHz and this allows the observation of ^{14}N lines which are of course much weaker than ^{35}Cl lines. Figure 6 obtained with a 1 s time constant shows the 3.407 MHz line obtained at 77 K from 715 mg (20 mmol of N) of hexamethylene tetramine (HMT) in a coil wound with fine wire on a 10 mm former 25 mm long which gives a sample

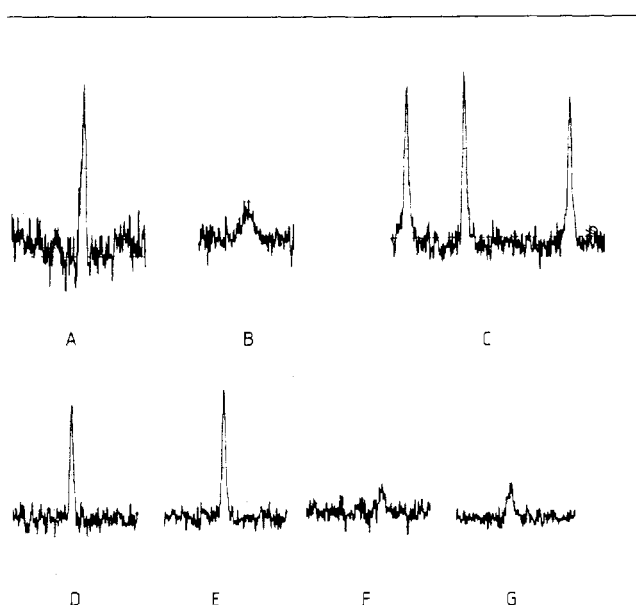


Figure 4. Lines obtained in a continuous scan from 55 to 27 MHz with a composite sample.

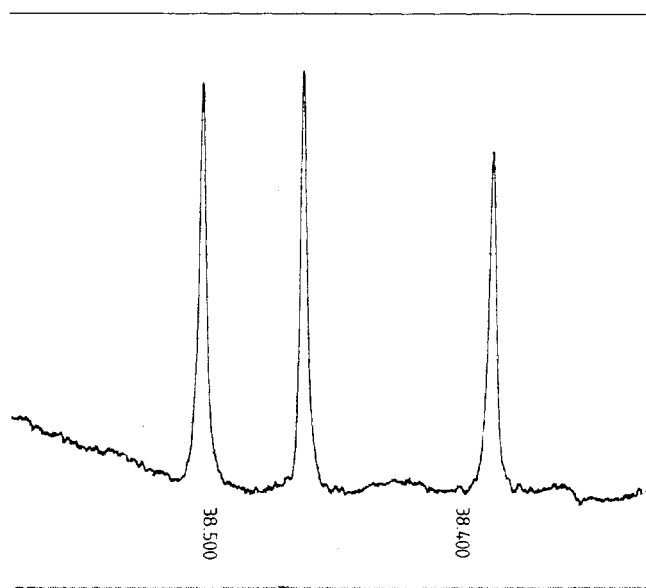


Figure 5. The spectrum of hexachlorobenzene at high resolution.

volume of $1.5\ \text{cm}^3$ by no means filled by the HMT. The signal-to-noise ratio is 18:1 and we have also observed the lines at 2.438 and 2.9125 MHz in 20 mmol of urea, which has an asymmetric field gradient, with a signal-to-noise ratio of 12:1.

The HMT result corresponds to a limiting sensitivity of about 1 mmol of nitrogen with a 1 s time constant so that this would give a useful line with a 10 s time constant and one might hope to detect nitrogen lines in compounds of molar volume up to $10^3\ \text{cm}^3$. Since nitrogen lines are easily saturated, it might be possible to improve the latter estimate by using a larger sample and coil. The direct resonance technique, though simpler and more flexible does not, of course, compare in sensitivity for low-frequency lines with the double resonance techniques developed by Edmonds and his colleagues (Edmonds *et al* 1974).

The high sensitivities that can be achieved mean that in many cases only very small samples will be required and this

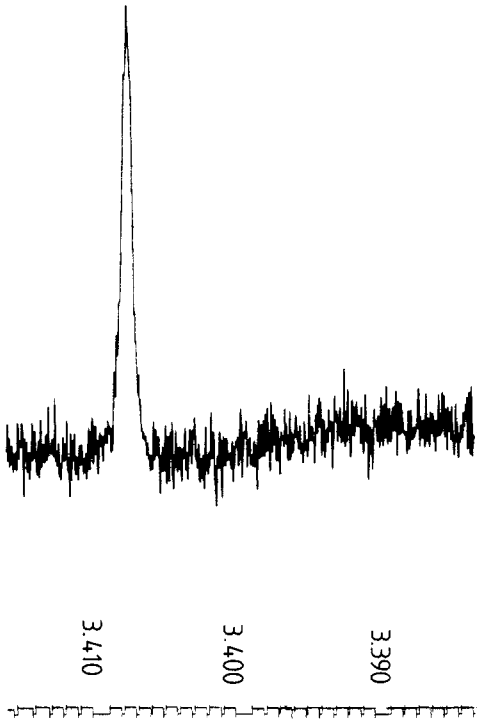


Figure 6. The nitrogen line in hexamethylene tetrammine.

extends the range of substances that can be studied and also means that only small single crystals will be needed for Zeeman studies. It also allows one, when searching for an unknown line, to incorporate a small sample of a standard material to act as a check on the spectrometer performance and as an aid to adjustment. If the standard sample frequency also has a well known dependence on temperature it can at the same time be used as a thermometer in direct contact with the main sample.

3. Theoretical sensitivity

If, in a coil of quality factor Q and effective volume U , we place a sample at a temperature T containing N_0 atoms giving a resonance of width $\Delta\nu$ at a frequency ν with a relaxation time T_1 , due to nuclei of isotopic abundance α , spin I and gyromagnetic ratio g , making transitions between the sublevels $\pm m$ and $\pm(m-1)$ and if we use a square-wave modulation scheme and a detector of bandwidth B and noise temperature T_n , then the signal-to-noise ratio predicted by Pound (1950) is, in SI units,

$$\frac{s}{N} = \frac{\mu_0^{1/2}}{6\pi} \alpha N_0 \left(\frac{g\beta h\nu^{3/2}(I+m)^{1/2}(I-m+1)^{1/2}}{kT(T_1\Delta\nu)^{1/2}(2I+1)} \right) \times \left(\frac{Q}{U} \right)^{1/2} \left(\frac{1}{kT_n B} \right)^{1/2} \quad (1)$$

where $\beta = 5.05 \times 10^{-27} \text{ J T}^{-1}$ is the nuclear magneton, h is Planck's constant and k is Boltzmann's constant. To achieve this limiting sensitivity the RF voltage V_1 across the tank circuit must satisfy

$$CV_1^2 \geq \frac{Uh^2\Delta\nu}{4\pi\mu_0 g^2 \beta^2 T_1} \quad (2)$$

where C is the tuning capacitance, otherwise the sensitivity is

less and cannot exceed

$$\frac{s}{N} = \frac{\mu_0}{3\pi} \alpha N_0 \left(\frac{g^2 \beta^2 h\nu^{3/2}(I+m)(I-m+1)}{kT\Delta\nu(2I+1)} \right) \times \left(\frac{Q^{1/2}}{U} \right) \left(\frac{2\pi CV_1^2}{kT_n B} \right)^{1/2} \quad (3)$$

These equations segregate, in separate brackets, terms which refer to the sample, the coil and the electronic circuit. The coil is described by Q and U and since Q is proportional to the coil diameter d while U varies as d^3 it is clear that when saturation is possible the signal for a fixed number N_0 of nuclei varies as $1/d$. When saturation is not possible it varies as $d^{-5/2}$ so that in either case the coil should be as small as possible. When, however, the nuclear density N_0/U is fixed, equation (1) gives a signal proportional to d^2 and now as much material as possible should be used in a coil just large enough to accommodate it. If this leads to a size where, according to equation (2), saturation is no longer possible the signal will finally increase only as $d^{1/2}$ so that to double the signal would then require 64 times as much material. It is also clear that in every case the sample volume should be as nearly equal to U as possible, i.e. a high filling factor is desirable and designs which sacrifice filling factor to other considerations will always lead to lower sensitivity. The circuit described here, by placing the coil near the tuning capacitor, leads to a high filling factor since there is little magnetic energy stored in the wire from the tank circuit to the active electronics.

In equation (3) the circuit is characterised by $V_1^2/T_n B$ and ideally we desire a value of V_1 which will saturate any resonance. In our circuit V_1 is restricted to less than 2 V which saturates almost any line in a coil of a few cm^3 volume at 77 K if not at room temperature. One could increase V_1 without degrading T_n at lower frequencies and this might possibly be worthwhile. However, sensitivity is most important when searching for a new line and this is best done at 77 K to take advantage of the increased Boltzmann factor so that henceforth we shall base our discussion on equation (1) rather than equation (3).

The bandwidth B is related (for a 6 dB roll-off) to the PSD time constant τ by $B = 1/4\tau$ and so we can reduce B , at the expense of taking longer to make a frequency scan, by increasing τ . The limit is set by the overall stability of the circuit which, in our case, corresponds to $\tau \sim 100$ s. This leaves only T_n to characterise the circuit and so, once the coil has been optimised, the over-riding consideration is a low noise temperature. To see how much room is left for improvement we consider three examples.

Line D in figure 4 is due to 370 μmol of chlorine at 77 K giving a line width of 1.5 kHz at 35 MHz with a relaxation time $T_1 = 1$ s. It was observed with $\tau = 1$ s and $B = 0.25$ Hz using a coil of measured $Q = 350$ and an effective volume $U = 3 \times 10^{-6} \text{ m}^3$ (3 cm^3). Equation (1) with $\alpha = \frac{1}{4}$, $g = 0.537$ and $I = m = \frac{3}{2}$ gives

$$s/N = 1.1 \times 10^{-18} N_0 / T_n^{1/2}$$

and since $N_0 = 223 \times 10^{18}$ and experimentally $s/N = 18$, this gives $T_n \sim 270$ K. Since 77 K arises from the tank circuit the electronic circuit contributes about 200 K, not far from the estimate obtained in § 4 from the circuit parameters. Certainly the electronic contribution is somewhere between 100 and 300 K and, even were we to eliminate it entirely, we would not increase s/N by more than about 2:1.

The small coil used to obtain the results shown in figure 3 has about $\frac{1}{2}$ the linear dimensions of the coil discussed above. We therefore expect the limiting sensitivity to be 5 μmol rather than 25 μmol . The measured value is better, 3 μmol . There are

two reasons; first the sample is different, sodium chlorate rather than p dichlorobenzene, and second the level was optimised to obtain figure 4 whereas figure 3 was obtained with the level set when the frequency was 55 MHz. This result is again consistent with an electronic noise temperature contribution between 100 and 300 K.

The nitrogen line in figure 6, with a signal-to-noise ratio of 18:1 at 77 K, was obtained, using a 1 s time constant and a coil with $Q=200$ and $U=2 \times 10^{-6} \text{ m}^3$, from 1.23×10^{22} nuclei with $g=0.403$, $I=m=1$, which give a line of width 900 Hz at 3.4 MHz and relaxation time $T_1=11 \text{ s}$. Equation (1) gives $s/N=1.28 \times 10^{-20} N_0/T_n^{1/2}$ and so we obtain $T_n \sim 77 \text{ K}$. It now looks as though most of the noise comes from the tank circuit and indeed at this frequency we expect the electronic contribution to be small, determined mainly by the FET input stage of the amplifier and certainly much less than 100 K.

It therefore appears that at 34 MHz there is room for a modest improvement but that at 3.4 MHz we are very nearly up against the theoretical limit. The most profitable avenue to explore would be to increase V_1 so that larger samples could be used at room temperature.

4. Circuit design

Figure 7 shows the basic circuit less a few of the bias components. Transistors 1 and 2 form a broadband mismatched pair amplifier (Cherry and Hooper 1963) and, if g_1 is the mutual conductance of T_1 , the gain is $A=g_1 R_2$ with a high-frequency roll-off mainly determined by the collector-base capacitance of T_2 , which is in parallel with R_2 . This amplifier has a low output impedance and drives the long-tailed pair T_3, T_4 . If the RF input to the base of T_3 has an amplitude exceeding about 100 mV the current through T_4 is switched on and off. A fraction (determined by C_1 and C_2) of this clipped current is fed back to the tank circuit and sustains oscillations whose amplitude is linearly proportional to the Q of the circuit and so responds directly to changes in Q due to NQR absorption. On the negative half-cycle T_3 is switched off, but on the positive half-cycle the current through T_3 continues to rise at a rate governed by R_3 , even after T_4 is off. Thus the collector current of T_3 contains a component which is a detected signal, and a RF input of amplitude v_1/π . To obtain stable oscillations it is essential that the transconductance from the base of T_3 to the drain of T_4 falls monotonically with increasing input and this requires that the ratio of the standing currents in T_3 and T_4 is between 3 and 0.3.

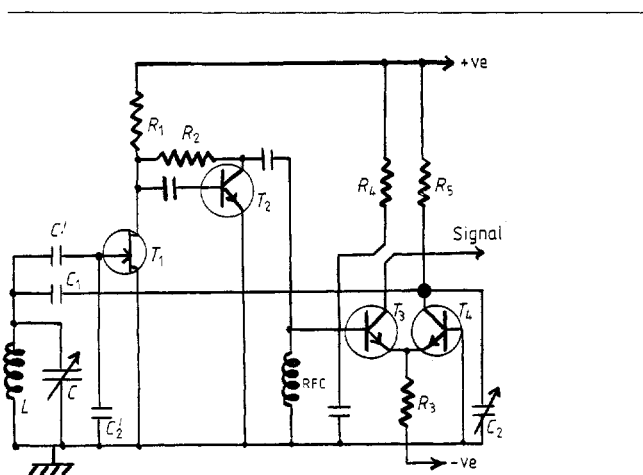


Figure 7. The basic circuit.

To ensure this the transistors are chosen so that their base-emitter voltages at the same current are matched to within a few millivolts and, to ensure monotonic detection at low levels, the transistor requiring the higher forward bias is used as T_3 .

At low levels the capacitive input impedance of T_3 has little effect on the pre-amplifier nor does it much affect the behaviour on the negative half-cycle. At higher levels, however, on the positive half-cycle, although the base-to-emitter admittance is reduced by the negative feedback due to R_3 (when T_4 is off) it is still necessary to charge the collector-base capacitance of T_3 . Now the long-tailed pair transistors are subject to two stringent requirements, they must have good high-frequency properties and also very low $1/f$ noise since this appears in the detected output of T_3 . The only satisfactory device that we have found is the PNP transistor type BCY71 which combines a high $f_t > 300 \text{ MHz}$ with very low $1/f$ noise. It has, unfortunately, about 6 pF collector-base capacitance and, at 50 MHz, this has a reactance of only 500 Ω . Thus to achieve a drive of 2 V or so to the limiter, T_2 must be able to swing over 4 mA and so must run with a standing current of about 8 mA. This problem, which limits the high-frequency performance, is, of course, quite insignificant below 20 MHz.

The typical shunt impedance Z of a tank circuit exceeds $10^4 \Omega$ which is much higher than the source impedance R_s that optimises the noise temperature of the amplifier and so the two input capacitors C_1' and C_2' (mainly the input capacitance of T_1) can be used to transform this impedance and the RF voltage to a lower value. With a step down ratio of 4:1 the input to T_1 is only 0.5 V when the RF voltage V_1 across the tank circuit is 2 V and it is this feature that allows us to achieve a reasonable tank circuit voltage without degrading the noise performance. In practice C_1' is about 2 pF and if the variable capacitor C_2 which sets the RF level has a maximum value of 60 pF the capacitor C_1 need only be 1 pF so that the entire circuit is very loosely coupled to the tank circuit with the advantages that we have mentioned in § 1.

Apart from Johnson noise in the tuned circuit the principal sources of noise are RF noise from the amplifier, low-frequency noise in the detector and RF noise fed back to the tank circuit from the collector of T_4 . Provided that $g_1 R_1$ exceeds about 3, the two significant sources of amplifier noise are those associated with T_1 and with the base current of T_2 . Noise in T_1 can be represented in terms of an equivalent noise resistance somewhat less than $2/3g_1$ and an equivalent noise conductance somewhat less than $\omega^2 C^2/3g_1$ where C is now the input capacitance of T_1 . Base current noise from T_2 increases the noise resistance by $g_2/2\beta g_1^2$, where g_2 is the mutual conductance and β the DC current gain of T_2 . The detector behaves as though it had an equivalent noise resistance $R_d' = \pi^2 R_n'$ where R_n' is the low-frequency noise resistance of the long-tailed pair. This is approximately equal to $R_3 + R_n$, where R_n is the noise resistance of T_3 at the detection frequency. The effects of $1/f$ noise are minimised because the base of T_4 is grounded and the base of T_3 returned to ground through a RF choke. For the transistor type BCY71 at 100 Hz $R_n = 250 \Omega$ over quite a wide range of emitter currents. Detector noise appears as an addition to the equivalent noise resistance which is therefore

$$r_n = \frac{2}{3g_1} + \frac{g_2}{2\beta g_1^2} + \left(\frac{\pi}{A}\right)^2 (R_3 + R_n), \quad (4)$$

but the noise conductance is unmodified

$$g_n = \frac{1}{3}\omega^2 C^2/g_1 \quad (5)$$

and these are associated with the usual reference temperature $T_0 = 293 \text{ K}$.

The main source of noise in the collector current of T_4 is Johnson noise from the 'tail' resistance R_3 and since this is only

connected half the time, the noise voltage developed across the tank circuit is

$$2kT_0dvZ^2\left(\frac{C_1}{C_1+C_2}\right)^2/R_3.$$

If I_0 is the standing current in each transistor and V_1 the RF voltage across the tank circuit, we have

$$V_1 = I_0 \left(\frac{C_1}{C_1 + C_2} \right) Z$$

and so the feedback noise contributes

$$T_f = \frac{1}{2} T_0 \left(\frac{V_1}{I_0} \right)^2 \frac{1}{ZR_3} \quad (6)$$

to the overall noise temperature of the system.

The contribution from the amplifier is

$$T_a = T_0 [(r_n/R_s) + R_s g_n]$$

and thus takes a minimum value

$$T_a = 2T_0 (g_n r_n)^{1/2}$$

if R_s is chosen to be

$$R_s = (r_n/g_n)^{1/2}.$$

The minimum is, however, very flat and an error 2:1 in R_s only increases T_a by 25%. We see that the minimum value of T_a due to the first stage alone is

$$T_a = \frac{2^{3/2}}{3} \frac{\omega C}{g_1} T_0 \sim \frac{\omega C}{g_1} T_0$$

and that this is modified, for the complete amplifier and detector, to

$$T_a \approx \frac{\omega C}{g_1} \left(1 + \frac{3g_2}{4\beta g_1} + \frac{3\pi^2}{2A^2} g_1 (R_3 + R_n)^2 \right)^{1/2} \quad (7)$$

which increases with R_3 whereas the feedback noise (6) decreases with R_3 . There is therefore an optimum value of R_3 . Rather than seek this rather flat optimum algebraically we consider a numerical example.

For the first field effect transistor T_1 we use the UHF type BF256LB with $g_1 \sim 4 \text{ mA V}^{-1}$ and $C \sim 3 \text{ pF}$. The second transistor is type MPSH11 which has a high f_c (650 MHz), a very low collector-base capacitance (less than 1 pF) and a reasonably high DC current gain $\beta > 50$ and it is run at 8 mA so that $g_2 \sim 320 \text{ mA V}^{-1}$. The value of R_2 in the high-frequency circuit is $10^3 \Omega$ so that $A=4$ and, with $R_n=250$ and $R_3=500 \Omega$, we obtain $r_n=830 \Omega$ of which more than half comes from the detector. For g_n at 30 MHz we have $2.7 \times 10^{-2} \text{ mA V}^{-1}$ and so the optimum source resistance is $R_s \sim 5.6 \times 10^3 \Omega$. A typical value for Z at this frequency is $35 \times 10^3 \Omega$ so that the input step down ratio should be about 2.5:1, although 4:1, by allowing a higher RF voltage with little change in T_a , might be better. The optimum value of T_a is 90 K. With $V_1=2 \text{ V}$, $I_0=1 \text{ mA}$, $R_3=500 \Omega$ and $Z=35 \times 10^3 \Omega$ we obtain $T_f \approx 40 \text{ K}$ giving an overall electronic contribution $T_e = T_a + T_f \sim 130 \text{ K}$. This, with the tank circuit at 77 K, gives a total noise temperature of about 200 K which is sufficiently close to our estimate 270 K, from the p-dichlorobenzene signal in figure 4, to give us confidence that our analysis is basically correct.

At lower frequencies we can increase R_2 and the amplifier gain, and decrease the current drawn by transistor 2. This virtually eliminates all the amplifier and detector noise except that due to transistor 1 and this is, in any case, small. Since the tank circuit impedance Z is also increased, which decreases the already small term T_f , it is not surprising that at 3 MHz the

measured noise temperature approaches the temperature of the tank circuit. As Z increases we can use a larger step-down ratio at the input without seriously increasing the noise, especially if the coil is at room temperature, and thus we can increase the RF level if necessary. Consider a 25 mm diameter coil at 3.4 MHz and at room temperature. We expect $Q \sim 200$ and, if this is tuned with a 100 pF capacitor, the shunt impedance is $Z \sim 9 \times 10^4 \Omega$. The noise resistance of the amplifier-detector will be about 200 Ω and the noise conductance quite negligible. Thus we could step Z down by 300:1 without much degrading the noise temperature and this would step the RF voltage down by 17:1 allowing the use of levels up to about 8 V. Although there would then only be 0.5 V RF at the input to T_1 , this would overload the detector T_3 and it would be necessary to reduce the gain by reducing R_2 .

We have so far assumed that the amplifier is not being overloaded but, although it is justifiable to regard it as fairly linear because of the negative feedback round T_2 , in fact both T_1 (a quadratic device) and T_2 (an exponential device), are being driven about half-way along their complete characteristics and are therefore appreciably non-linear at high levels. As a result $1/f$ noise generated by T_1 and especially by T_2 can modulate the RF carrier and seriously degrade the noise performance. To avoid this these transistors are biased using large resistors (R_6 and R_7 in the complete circuit shown in figure 8) in their source and emitter leads and also a -27 V negative supply rail. These bias resistors are only bypassed by small capacitors, of negligible reactance at RF but high reactance near 100 Hz and so both T_1 and T_2 have considerable negative feedback (26 dB for T_1 and 60 dB for T_2) at low frequencies. This reduces the low-frequency noise voltage between the gate and source, or base and emitter, and so minimises cross modulation.

The Zeeman modulating field, especially if it is coaxial with the RF coil, can generate voltages in this coil at odd harmonics of the modulation frequency of the order of several mV. This pick up, though it is ignored by the PSD, can easily overload the circuit. It is therefore eliminated, see figure 8, by placing a RF choke from the gate of T_1 to ground. If $C_1=3 \text{ pF}$ and the choke inductance is as large as 2 mH the pick up is reduced by approximately 10^{-8} . This choke and also the choke used at the input to the limiter can themselves pick up the modulation. They therefore take the form of two very small ferrite-cored chokes in series, mounted in the PCB as an astatic pair.

The signal and noise level at the output of the detector transistor T_3 is relatively large, the noise is about 50 nV per root Hz, and so the noise figure of the LF amplifier is not critical; however, by including this amplifier, with a voltage gain of about 100, in the RF box the signal is raised to a level where pick up in the output lead can be ignored as well. A buffer RF amplifier is also used to isolate the circuit from pick up on the lead to the frequency counter.

Finally the outputs of integrated circuit power supply stabilisers usually exhibit several hundred microvolts of noise and also occasional spikes due to transients on the mains. These can be partially eliminated by simple RC filtering outside the RF box but in practice we have found it most satisfactory to place a further transistorised filter in the box itself. With these precautions there is very little trouble from extraneous noise though, to be on the safe side, we use a basic modulation frequency of 87 Hz so that the detected second harmonic at 174 Hz is as far away as possible from harmonics of the 50 Hz mains.

5. Practical circuit

Figure 8 shows the complete circuit including the varicap (BB105) bandspread circuit, the RF buffer amplifier T_5 (BFX89),

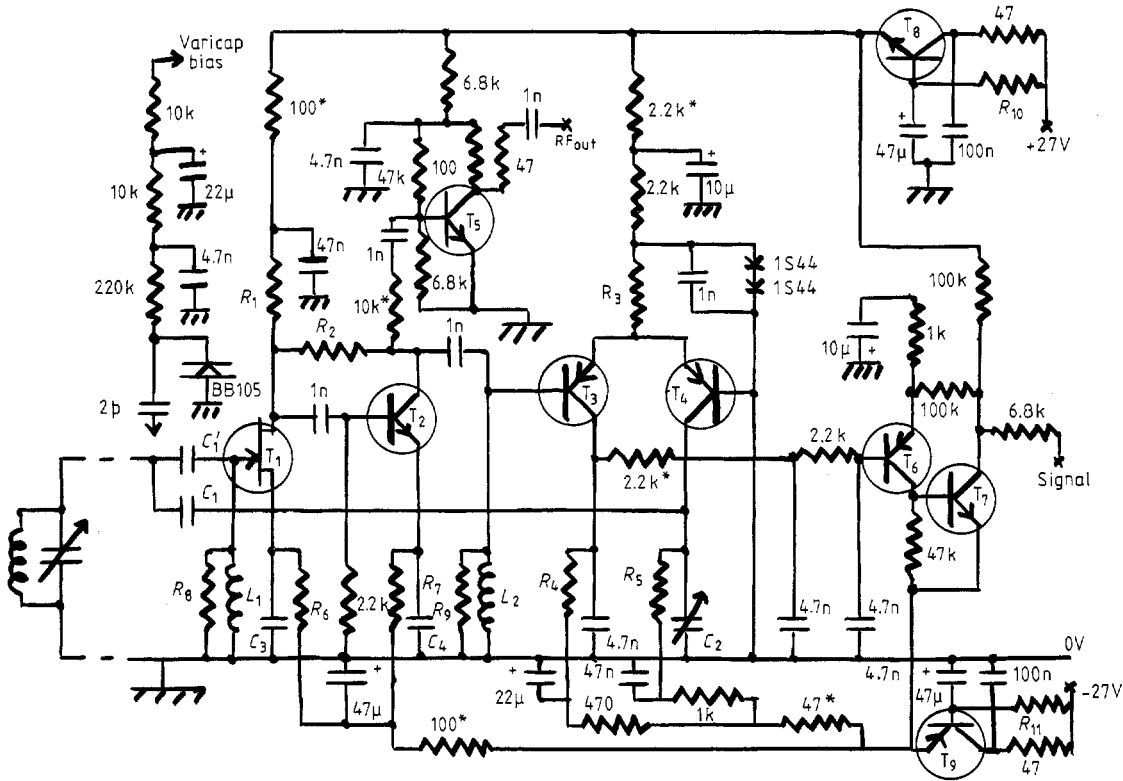


Figure 8. The complete circuit.

the supply line filters T_8 (BC182L) and T_9 (BC212L), and the LF buffer amplifier T_6 (BCY71) and T_7 (BC182L). The values of the unmarked components (with the LF version values in brackets) are: $L_1=L_2$, an astatic pair of $33\ \mu\text{H}$ (1 mH) sub-miniature RF chokes, Sigma type SC 30; $R_1=680\ \Omega$ (1 k Ω), $R_2=1\ \text{k}\Omega$ (4.7 k Ω), $R_3=470\ \Omega$, $R_4=8.2\ \text{k}\Omega$, $R_5=15\ \text{k}\Omega$, $R_6=4.7\ \text{k}\Omega$, $R_7=3.3\ \text{k}\Omega$ (10 k Ω), $R_8=33\ \text{k}\Omega$ (100 k Ω), $R_9=3.3\ \text{k}\Omega$ (10 k Ω), $R_{10}=15\ \text{k}\Omega$ (22 k Ω), $R_{11}=22\ \text{k}\Omega$ (33 k Ω). C_1 and C_1' are fabricated by wrapping 0.25 mm wire over a 2 mm

wire sleeved with PTFE tubing, C_3 is 4.7 nF in parallel with 68 pF. C_4 is $2 \times 4.7\ \text{nF}$ (4.7 nF + 47 nF) in parallel with 68 pF and C_2 is a Mullard type 800 miniature trimmer. All the resistors are miniature metal film (Mullard type MR25), most of the capacitors up to 4.7 nF are Mullard miniature plate ceramics though the 1 nF capacitors coupling T_2 to T_3 and T_5 to the RF output lead are polystyrene. The 47 nF and 100 nF capacitors are polyester and the electrolytic capacitors are miniature PCB mounting types, rated at 35 V.

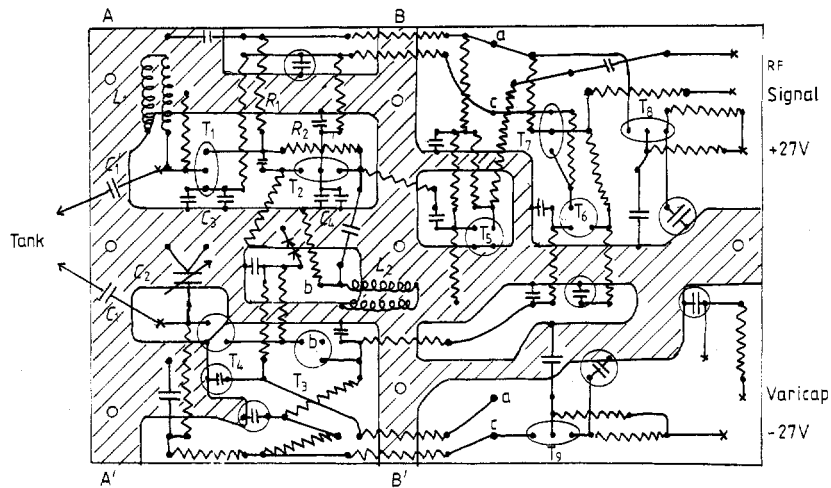


Figure 9. Printed circuit board layout.

The values of the bias and load resistors associated with T_1 and T_2 are chosen so that the collector of T_2 is at about +7 V and the drain of T_1 at +15 V and since the mutual conductance of T_1 (BF256LB) is 4 mA V^{-1} the gain of the HF amplifier is 4 and in the LF version 20. With $R_3 = 470 \Omega$ the bias required by T_3 and T_4 to give 0.8 mA each is about +1.4 V and this is obtained by driving 5 mA forward current through two small diodes, 1S44, in series. The load R_5 is chosen to leave the collector of T_4 at about -12 V and the 8.2 k Ω load R_4 causes the collector of T_3 to rise from -18 at zero RF level to about -8 V at maximum level. The buffer amplifier T_6T_7 has a gain of 100 above 100 Hz and unity gain for DC. Thus the DC level of the signal output rises from about -16 V to -6 V as the RF level increases. A 100 μA FSD meter with a total series resistance of 100 k Ω , including the potentiometer used to back off the zero level, is used to monitor this voltage and the resistance is split into equal parts with a capacitor (10 μF) to ground at the centre point, to prevent interference picked up by the meter from entering the signal input to the PSD.

The whole circuit is built on a glass fibre PCB (89 mm \times 58 mm) and since the layout of the oscillator components is critical a diagram of this board is shown in figure 9. The view is from the copper-clad side and the components (transistors, resistors, capacitors etc) on the other side of the board are shown as though it were transparent. Dots mark the holes where the components are attached, crosses mark circuit pins to which C_1 , C_f and the output leads are attached. The copper ground plane is shown hatched, a link below the copper side joins bb (the base lead of T_3) and two links behind the board aa and cc complete the positive and negative supply rail wiring. Electrolytic capacitors and the transistors are ringed. Two $\frac{3}{16}$ " square aluminium alloy bars are bolted by three screws across the board at AA' and BB'. These and a $\frac{1}{16}$ " post at C support the PCB from the bottom of the diecast box. The bar BB' separates the oscillator from the rest of the circuit since above the PCB it is only traversed by resistors (shown asterisked in figure 8). Two slots are machined in the bottom of the bar AA', where it bolts to the box, to allow return currents from the tank circuit a direct access to the copper ground plane of the PCB. Figure 10 shows the PCB mounted in the box. The varicap circuit is omitted but it bolts to the end of the box near where the RF lead from the tank coil enters the box.

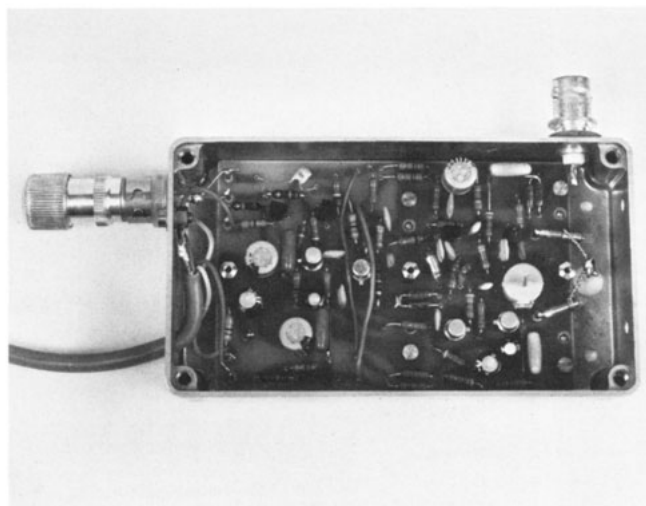


Figure 10. The circuit in place in its case.

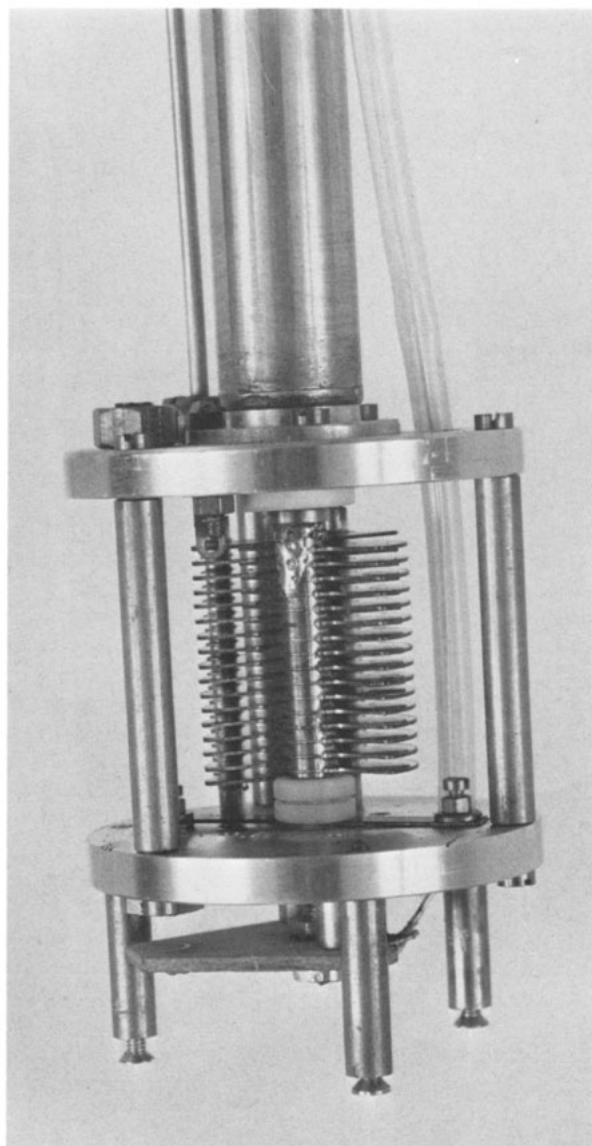


Figure 11. The tuning capacitor.

6. The tuning capacitor

Making a tuning capacitor which would run freely at 77 K without contact noise and which had a large ratio of maximum to minimum capacitance proved to be the most difficult task in the whole design. The solution is shown in figure 11. The capacitor is constructed using the rotor and stator from a Jackson Bros. air-spaced 150 pF trimmer type C8. The stator is grounded to the support frame and the rotor runs between two ball bearings, with $\frac{3}{16}$ " nylon balls in PTFE races, which are lightly loaded by a phosphor-bronze leaf-spring. A 3 mm hole is bored 25 mm deep into the end of the rotor shaft remote from the drive and into this hole is inserted a thin (1.5 mm \times 0.1 mm) copper tape sheathed in a thin-walled PTFE tube. The tape is soldered to the rotor through a small side hole at the bottom of the bore, and the other end is fixed to an insulating support to form the 'live' lead to the coil. With stops to restrict the rotor movement to 180° the tape is never twisted by more than 90° and, since it is only 1.5 mm wide and 30 mm long, its life is indefinite.

The stator is fixed to the end plates by brass grub screws, and this allows its position to be adjusted after the rotor

assembly has been put together. The drive shaft of the rotor is coupled through a short length of nylon rod and a Heli-Cal (R) universal joint to a longer length of nylon rod which in turn is coupled by a universal joint to the final drive shaft from the worm gear. This gives a structure that maintains its alignment and runs smoothly over a wide temperature range, and no jitter due to either contact noise or stiffness in the bearings is observed as the capacitor is tuned. The capacitor frame is supported from the cryostat top plate by a 15 mm stainless steel tube concentric with the drive shaft, and at the bottom of the frame a circular plate (not shown) carries the thin-walled copper tube containing the sample coil.

A cover, with spring fingers, fits over the capacitor and gives good thermal contact with the cryostat walls as well as a solid earth return contact. A single silver-plated stainless steel wire leads from the live terminal of the capacitor to the RF feedthrough bush in the top plate.

7. Adjustment

The capacitor C_1 is first chosen roughly to match the expected shunt impedance of the coil to the amplifier, to give the minimum noise figure. The input capacitance of the amplifier, including strays, is about 5 pF so that $C_1 = 2$ pF gives a 2:7 step down ratio. It is better to make C_1 smaller rather than larger than the first rough estimate since this allows the RF level to be higher without much degradation of the noise figure. In practice the value of C_1 is not very critical. A signal generator can then be connected between the tank circuit terminal and ground, to calibrate the level meter. The feedback capacitor C_2 is chosen next, so that with C_2 at its maximum value the lowest level desired at the highest frequency can be obtained. The circuit is then ready for use and will need no further adjustment, except setting C_2 , unless the tank coil is changed to one of radically different inductance and Q . It is now only necessary to set the modulator and PSD controls and choose a sweep rate.

The only troublesome source of interference that we have experienced comes from switching transients produced by the counter on certain ranges. These get into the RF circuit by radiation, not down the cable, since they are present when this cable is disconnected and the counter is driven by a signal generator. They are easily eliminated by choosing a different counter range.

8. The power supply, etc

The ± 27 V supplies are obtained using 100 mA, 24 V integrated stabilisers boosted to 27 V by diodes in the common leads and this PSU is housed in a separate case. A second case houses the level meter, the sweep unit for the varicap diode and two RC filters (47 Ω , 1000 μ F) to remove spikes and most of the noise from the supply rails.

The phase-sensitive detector has one novel feature. Although we have interpreted our results in terms of the usual 6 dB per octave RC integrator we actually use a linear integrator described by Grimbleby (1980) since for a given bandwidth this gives a faster response. Apart from a change in the resistance and capacitance values to give time constants up to 500 s this follows his circuit exactly although it is realised using a single quadruple operational amplifier LM324.

With the final mechanical reduction gear (100:1) rigidly attached to the cryostat the mechanical drive to this gear from the motor presents no problems and vibration is easily eliminated using three standard flexible couplings. It is however, important to ensure that the shaft to the capacitor does not bind where it passes through the O ring seal; this is therefore rather carefully machined so that the radial clearance between the shaft and the bore is only slightly (2%) less than the chord of the O ring. In order to prevent the ingress of moisture past this rather

leaky seal the interior of the cryostat is maintained at a slight overpressure of helium. Air is not suitable and even with helium it is possible to cause a measurable change in the oscillator frequency by changing the pressure, despite helium's very low dielectric susceptibility.

Although our modulator will provide up to 2 A at 30 V with a variable frequency we rarely use more than 10% of this output and since there appears to be little change in the signal-to-noise ratio with modulation frequency this is usually left set at 87 Hz. We have also found very little difference in the spectra obtained with transverse fields produced by a coil, such as that shown in figure 1, and axial coils. The latter are more compact and have less ohmic loss than the transverse coils and if a 1 mm radial clearance is left between the tail of the cryostat and the coil former, the coolant liquid can circulate freely over the tail. It is not necessary to obtain a uniform modulating field, indeed, a non-uniform field reduces the spurious inverted wings on the lines so that we frequently place the coil so that the specimen is only in the fringing field at the end of the coil.

8. Conclusion

We have shown that it is possible to construct a cw spectrometer which, despite its rather limited RF level, gives high sensitivity, both in terms of sample size and acceptable molar volume, by virtue of its low noise temperature. Temperatures from 77 K to 80°C are accessible with a simple cryostat and there is no reason why, with a more elaborate cryostat, one should not reach lower temperatures. Above room temperature there is little advantage in placing the capacitor near the coil since this will not have a very high Q and the line from the coil to the rest of the system can be kept short. With available devices there is little prospect of extending the upper frequency limit of this circuit much above 100 MHz and, in a forthcoming paper, we shall describe a rather different system for use up to 700 MHz.

Although we have discussed the circuit solely in terms of pure NQR it can, of course, also be used as a sensitive NMR spectrometer. For example, Bleaney *et al* (1982) have recently used it to study not only the zero-field resonance of the common isotope ^{51}V in SmVO_4 at temperatures between 1.6 and 4.2 K, but also the quadrupole splitting of the NMR lines due to ^{51}V and the rare (0.24% abundant) isotope ^{50}V . Their measurements give the ratio of the two quadrupole moments $^{50}Q/^{51}Q = 4.019$ (4) with an accuracy five times better than earlier measurements.

References

- Bleaney B, Gregg J F and Wells M R 1982 The ratio of the nuclear electric quadrupole moments of ^{50}V and ^{51}V in SmVO_4 *J. Phys. C: Solid St. Phys.* **15** L349
- Cherry E M and Hooper D E 1963 The design of wide-band transistor amplifiers *Proc. IEE* **110** 375
- Edmonds D T, Hunt M J, Mackay A L and Summers C P 1974 The high sensitivity detection of pure NQR *Adv. Nucl. Quadrupole Resonance* **1** 145
- Faulkner E A and Holman A 1967 An improved circuit for nuclear magnetic resonance *J. Sci. Instrum.* **44** 391
- Fitzky H G 1974 NQR resonance spectroscopy for analysis of chlorinated organic compounds in industry *Adv. Nucl. Quadrupole Resonance* **1** 79
- Grimbleby J B 1980 Averaging filter circuits for signal recovery applications *J. Phys. E: Sci. Instrum.* **13** 557

A sensitive nuclear quadrupole resonance spectrometer

Pound R V 1950 Nuclear electric quadrupole interactions in crystals

Phys. Rev. **79** 685

Robinson F N H 1959 Nuclear resonance absorption circuit
J. Sci. Instrum. **36** 481

Robinson F N H 1974 *Noise and Fluctuations* (Oxford: Oxford University Press)

Robinson F N H 1980a Base-line drift in NQR spectrometers
J. Magn. Resonance **39** 155

Robinson F N H 1980b A bi-symmetric Zeeman modulator for nuclear quadrupole resonance
J. Phys. E: Sci. Instrum. **13** 961

Verwieck J F and Cornwell C D 1961 Radio-frequency spectrometer with bidirectional wave frequency modulation
Rev. Sci. Instrum. **32** 1383

Watkins G D and Pound R V 1952 The pure nuclear electric quadrupole resonance of N^{14} in three molecular solids
Phys. Rev. **85** 1062

Weaver J R M and Robinson F N H 1981 NQR of bismuth and the quadrupole Hamiltonian
Phys. Lett. **85A** 389